Departmental Papers (MSE)   Department of Materials Science & Engineering

November 2001

Local Polarization, Charge Compensation, and Chemical Interactions on Ferroelectric Surfaces: a Route Toward New Nanostructures

Dawn A. Bonnell
University of Pennsylvania, bonnell@lrsm.upenn.edu

Sergei V. Kalinin
University of Pennsylvania

Follow this and additional works at: http://repository.upenn.edu/mse_papers

Local Polarization, Charge Compensation, and Chemical Interactions on Ferroelectric Surfaces: a Route Toward New Nanostructures

Abstract

The local potential at domains on ferroelectric surfaces results from the interplay between atomic polarization and screening charge. The presence of mobile charge affects surface domain configuration, switching behavior, and surface chemical reactions. By measuring the temperature and time dependence of surface potential and piezo response with scanning probe microscopies, thermodynamic parameters associated with charge screening are determined. This is illustrated for the case of $BaTiO_3$ (100) in air, for which the charge compensation mechanism is surface adsorption and enthalpy and entropy of adsorption are determined. The local electrostatic fields in the vicinity of the domains have a dominant effect on chemical reactivity. Photoreduction of a large variety of metals can be localized to domains with the appropriate surface charge. It has been demonstrated that proximal probe tips can be used to switch polarization direction locally. Combining the ability to 'write' domains of local polarization with domain specific reactivity of metals, vapors of small molecules, and organic compounds leads to a new approach to fabricating complex nanostructures.

Local Polarization, Charge Compensation, and Chemical Interactions on Ferroelectric Surfaces: a Route Toward New Nanostructures

Dawn A. Bonnell and Sergei V. Kalinin
Dept. Mat. Sci. Eng., University of Pennsylvania, 3231 Walnut St,
Philadelphia, PA 19104

ABSTRACT

The local potential at domains on ferroelectric surfaces results from the interplay between atomic polarization and screening charge. The presence of mobile charge affects surface domain configuration, switching behavior, and surface chemical reactions. By measuring the temperature and time dependence of surface potential and piezo response with scanning probe microscopies, thermodynamic parameters associated with charge screening are determined. This is illustrated for the case of $BaTiO_3$ (100) in air, for which the charge compensation mechanism is surface adsorption and enthalpy and entropy of adsorption are determined. The local electrostatic fields in the vicinity of the domains have a dominant effect on chemical reactivity. Photoreduction of a large variety of metals can be localized to domains with the appropriate surface charge. It has been demonstrated that proximal probe tips can be used to switch polarization direction locally. Combining the ability to 'write' domains of local polarization with domain specific reactivity of metals, vapors of small molecules, and organic compounds leads to a new approach to fabricating complex nanostructures.

INTRODUCTION

Development of spontaneous polarization and related lattice distortion below the Curie temperature in a ferroelectric material results in the formation of regions of uniform polarization, i.e. ferroelectric domains. Polarization discontinuities in the vicinity of surfaces and interfaces result in polarization bound charge that significantly affects materials properties. Polarization charge can compensate Schottky barriers at the interfaces giving rise to Positive Temperature Coefficient of Resistance behavior in semiconducting $BaTiO_3$. In the vicinity of surfaces, polarization charge results in domain specific adsorption of charged species from the ambience that effectively compensates the charge, i.e. extrinsic screening processes [1]. Screening charges thus affect the thermodynamic properties of a ferroelectric surface via a reduction in depolarization energy. Therefore, screening plays a significant role in the polarization reversal processes and, to a large extent, determines the stability of domain structures in ferroelectric materials. Another type of screening process involves band bending in the near surface region (intrinsic screening) with the formation of depletion and accumulation layers depending on the nature of majority charge carriers in the ferroelectric semiconductor. These domain specific space charge layers strongly influence local chemical activity of ferroelectric surfaces as discovered by Giocondi and Rohrer [2,3]. Studies of domain specific chemical phenomena are hindered by typical multidomain structure of the samples. Until recently, only limited progress has been achieved in the understanding of the effects of local polarization on adsorption and chemical reactivity of ferroelectric surfaces due to the lack of appropriate characterization techniques.

The current tendency towards the miniaturization of ferroelectric based electronic components [4,5] has motivated a number of scanning probe microscopy (SPM) studies of ferroelectric materials. SPM provides information on the topographic features, the potential and field above the surface, and local electromechanical properties. Non-contact techniques such as Scanning Surface Potential Microscopy (SSPM) and Electrostatic Force Microscopy (EFM) are sensitive to electrostatic fields, which for ferroelectric surfaces have contributions from both polarization and screening charge [6].

In the present paper, SPM was used to study domain related chemical activity of ferroelectric surfaces in adsorption and photochemical deposition processes. Variable temperature SSPM is used to determine the temperature and time dynamics of effective surface potential on $BaTiO_3$ surfaces. A thermodynamic model based on the Ginzburg-Devonshire theory is developed that allows enthalpy and entropy of adsorption to be determined from equilibrium potential contrast. Piezoresponse force microscopy (PFM) is used to determine domain patterns in polycrystalline $BaTiO_3$ and correlate them with metal photodeposition pattern. This technique provides a new approach towards the generation of nanometer scale structures.

EXPERIMENT

Thermodynamic of adsorption

The AFM and SSPM measurements were performed on a commercial instrument (Digital Instruments Dimension 3000 NS-III) using metal coated tips ($l \approx 225$ μm, resonant frequency ~ 60 kHz, $k \approx 1$ N/m). The lift height for the interleave scans in SSPM was 100 nm, the scan rate was typically 1 Hz and amplitude of the driving voltage, V_{ac}, was 5 V. Variable temperature measurements were performed on a home-built heating stage. During measurements, the temperature was increased in steps of ~10°C. Several images were acquired at ~10 min intervals at each temperature. The cantilever was re-tuned at each step in order to stay in the vicinity of the resonance frequency. Thermal drift was corrected by adjusting lateral offsets to position domain-unrelated topographical features. Topographic images were processed by line (first order) flattening to remove the effect of surface tilt and noise in slow scan direction. SSPM images acquired at room temperature were processed only by plane subtraction. During variable temperature measurements higher levels of thermal noise necessitated zero order flattening.

A barium titanate (100) single crystal (5x5x1 mm, $T_c = 130$°C, Superconductive Components, Inc) was used for the experiment. The roughness of the (100) face did not exceed 15 Å. Prior to analysis the crystal was repeatedly washed in acetone and deionized water. In order to obtain a reproducible well-developed domain structure the crystal was heated above the T_c, held at 140°C for ~0.5 h and cooled on a metallic surface.

Domain selective photochemical deposition

$BaTiO_3$ samples were prepared by sintering commercial $BaTiO_3$ powder (Aldrich). Powders were ball-milled and pressed into pellets, which were annealed for 12h at 1400°C. Samples were cut with a diamond saw and exposed surfaces were polished with SiC media down to 1 μm grit size and by alumina down to 50 nm size. Samples thus obtained were thermally etched at 1400°C for 12 h, producing grain boundary grooving and surface faceting, which provide a clear topographic contrast that can be used as markers in AFM experiment. This procedure is also crucial to relieve surface damage associated with polishing. PZT thin films

were prepared by a sol-gel method on Pt/Si substrates. The film thickness was ~200 nm and characteristic grain size was 50-100 nm.

The contact-mode AFM and PFM measurements were performed on a commercial instrument (Digital Instruments Dimension 3000 NS-III). For piezoresponse measurements, the AFM was additionally equipped with a function generator and lock-in amplifier (DS340, SRS 830, Stanford Research Systems). Pt coated tips (l ≈ 125 μm, resonant frequency ~ 350 kHz) (Micromasch NSCS12 Pt) were used for these measurements. To perform polarization switching in polycrystalline $BaTiO_3$, the microscope was equipped with a PS310 high voltage power supply (Stanford Research Systems). The electrical connections between the microscope and the tip were severed and a wire was connected from the function generator to the tip through a custom-build sample holder. This set-up allowed dc voltages up to 150 V_{dc} to be applied to the tip. Modulation amplitude in the PFM imaging was 6 V_{pp}; larger amplitudes resulted in polarization reversal in the metastable switched regions.

To pattern domains, the function generator output was controlled through the GPIB interface using in-house control software [7]. After scanning a selected region, the tip was ac biased and scanned over larger region, thus allowing the switched domain to be imaged. Polarization in PZT samples can be switched by voltages as low as 5-10 V_{dc}. Polarization switching in $BaTiO_3$ ceramics requires high voltages (100V_{dc}).

For silver photodepositon, samples were placed in the 0.01 M $AgNO_3$ solution and irradiated by Xe UV lamp for 10 s at 100W. After deposition samples were washed and dried by air flow. Deposition conditions are specific for individual cations, e.g. Pd requires longer exposure time (~30 min from 0.01M $PdCl_2$ solution).

THEORETICAL TREATMENT OF SCREENING

Thermodynamics of partially screened ferroelectric surface

The surface of a ferroelectric material is characterized by a polarization charge density $\boldsymbol{s} = \mathbf{P} \cdot \mathbf{n}$, where $\mathbf{P}$ is the polarization vector and $\mathbf{n}$ is the unit normal to the surface. However, the unscreened state is unstable and extrinsic surface adsorption and/or intrinsic charge redistribution result in polarization screening at ferroelectric surfaces or interfaces [1]. In the case when charge compensation is due to adsorption, the free energy for screening process is:

$$E(\boldsymbol{a},T) = E_{el}(\boldsymbol{a},T) + \boldsymbol{a}\frac{P}{qN_a}\Delta H_{ads} - \boldsymbol{a}\frac{P}{qN_a}T\Delta S_{ads} \qquad (1)$$

where $q = 1.602 \cdot 10^{-19}$ C is electron charge, P is spontaneous polarization, $N_a = 6.022 \cdot 10^{23}$ mol^{-1} is Avogadro number, $\boldsymbol{a}$ is the degree of screening and T is the temperature [8]. The enthalpy and entropy of adsorption are denoted ΔH_{ads} and ΔS_{ads}, respectively. The electrostatic contribution to the free energy in Eq. (1), $E_{el}(\boldsymbol{a},T)$, is:

$$E_{el}(\boldsymbol{a},T) = \frac{P^2}{\boldsymbol{e}_0 + \sqrt{\boldsymbol{e}_x \boldsymbol{e}_z}}\left\{(1-\boldsymbol{a})^2 L \frac{7\boldsymbol{z}(3)}{2\boldsymbol{p}^3} + \boldsymbol{a}h\frac{\boldsymbol{e}_0}{\boldsymbol{e}_2} + \boldsymbol{a}^2 h\frac{\sqrt{\boldsymbol{e}_x \boldsymbol{e}_z}}{\boldsymbol{e}_2}\right\}, \qquad (2)$$

where L is the domain size, h is the screening layer width, $\boldsymbol{e}_2$ is the dielectric constant of the screening layer, $\boldsymbol{e}_x$ and $\boldsymbol{e}_z$ are the dielectric constants of the ferroelectric and $\boldsymbol{e}_0 = 8.854 \cdot 10^{-12}$ F/m is the dielectric constant of vacuum. The temperature dependence of the equilibrium screening can be obtained from the condition of the minimum of free energy $\partial E(\boldsymbol{a},T)/\partial \boldsymbol{a} = 0$.

Since $E_{el}(\boldsymbol{a},T)$ is a quadratic function of α [Eq.(2)], this condition can be written as $\partial E(\boldsymbol{a},T)/\partial \boldsymbol{a} = a_1(T)\boldsymbol{a} + a_2(T)$. Thus, from Eqs. (1,2) the equilibrium degree of screening is

$$\boldsymbol{a}(T) = T\frac{P}{qN_a}\frac{\Delta S_{ads}}{a_1(T)} - \frac{P}{qN_a}\frac{\Delta H_{ads}}{a_1(T)} - \frac{a_2(T)}{a_1(T)} \tag{3}$$

where $a_1(T)$ and $a_2(T)$ are temperature dependent coefficients defined by domain structure and material properties. The temperature dependencies of $a_1(T)$, $a_2(T)$ are calculated within the framework of the Ginzburg-Devonshire [9-11] theory and these values are shown to be only weakly temperature dependent [8].

SSPM Contrast vs. Degree of Screening

The effective potential measured by SSPM contains contributions both from screened and unscreened components of polarization charge. The force acting on the biased tip above a partially screened ferroelectric surface is written as a sum of capacitive and Coulombic components. In SSPM the tip bias is $V_{tip} = V_{dc}+V_{ac}\cos(\boldsymbol{w}t)$, where V_{ac} is driving voltage and the first harmonic of the force is:

$$F_{1\boldsymbol{w}} = \frac{dC}{dz}(V_{tip} - V_s)V_{ac} + CV_{ac}E_z \tag{4}$$

where $C = C(z)$ is the distance dependent tip-surface capacitance, V_{tip} is the tip bias, V_s is the surface potential due to electric double layer, and E_z is the normal component of electric field due to unscreened polarization charge. To quantify the capacitive and Coulombic components of the tip-surface interactions, a line charge model is used. For a typical metal coated tip used in the SSPM measurements with $\boldsymbol{q} = 17°$, $H \approx 10$ μm and tip-surface separation $z = 50\text{-}100$ nm effective potential difference between the domains is

$$\Delta V_{dc} = (V_1 - V_2) - 1.18H(E_1 - E_2) \tag{5}$$

where V_1, V_2 and E_1, E_2 are potential and field above domains of opposite polarity.

Using the representation of a partially screened ferroelectric surface as a sum of completely unscreened and completely screened part, the potential difference between domains of opposite polarity is $\Delta \boldsymbol{j}_s = \boldsymbol{a}\, 2h\sqrt{\boldsymbol{e}_x \boldsymbol{e}_z}\,P/\boldsymbol{e}_2(\boldsymbol{e}_0 + \sqrt{\boldsymbol{e}_x \boldsymbol{e}_z})$, while the difference in the normal component of the electric field is $\Delta E_u = (1-\boldsymbol{a})P/(\boldsymbol{e}_0 + \sqrt{\boldsymbol{e}_x \boldsymbol{e}_z})$. Therefore, domain potential contrast is a linear function of degree of screening. Combination of Eq. (3) and Eq. (5) thus suggests that the surface potential difference between the domains as measured by SSPM is a linear function of temperature as well. Therefore, the temperature dependence of domain potential contrast can be used to estimate the temperature dependence of the degree of screening and determine thermodynamic parameters associated with the screening process.

RESULTS AND DISCUSSION

Kinetics and thermodynamics of screening process

The domain structure of the BaTiO$_3$ (100) surface is shown in Fig. 1. Surface topography indicates the presence of 90° a-c domain walls. The SSPM image indicates the presence of domains of opposite polarity within c domains. A detailed analysis of domain structure from the combination of AFM and SSPM data is discussed elsewhere [6]. On increasing the temperature the domain structure does not change significantly. Neither 90° nor 180° domain wall motion is
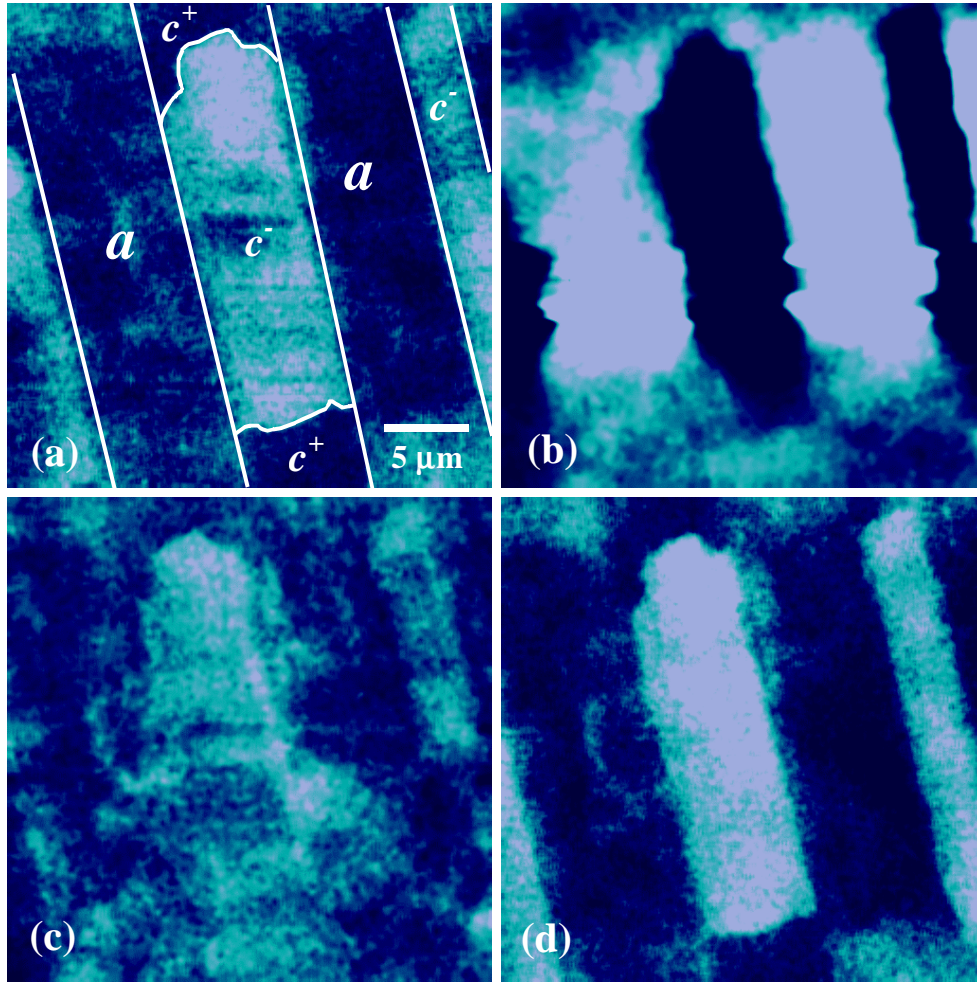
Figure 1. Surface potential (a) of ferroelectric domain structure on BaTiO$_3$ (100) surface at T = 90°C. Surface potential during cooling from 90°C to 70°C (b), at 70°C (c) and after annealing at 70°C for 50 min (d). Streaks on (b) are due to the significant vertical displacements of the surface during cooling. Note that the sign of surface potential features inverts on cooling. On lowering the temperature the spontaneous polarization increases and for a short period of time polarization charge dominates over screening charge in the potential image. At constant temperature screening charges adsorb on the surface, domain contrast passes through the isopotential point (c) and after equilibration the sign of domain potential is again determined by the screening charges (d).

observed. After a temperature decrease from 70°C to 50°C the domain contrast inverts (Fig. 1a,b), i.e. a positive c domain becomes negative. The potential difference between the domains decreases with time, passing through an isopotential point corresponding to zero domain potential contrast (Fig. 1c), and finally establishing an equilibrium value (Fig. 1d).

This phenomenon, which will be referred to as temperature induced domain potential inversion, is consistent with the proposed explanation of screening on ferroelectric surfaces. In the case of complete screening, the surface potential has the sign of the screening charges and is reverse to that expected from polarization orientation, i.e. c^+ domains are negative and c^- domains are positive on the SSPM image. Increasing the temperature results in a decrease of polarization bound charge leaving some of the screening charge uncompensated, thus increasing the effective surface potential. On decreasing the temperature spontaneous polarization increases

and, for a short period of time, the sign of domain potential is determined by the polarization charge. Under isothermal conditions, polarization and screening charges equilibrate and the potential establishes an equilibrium value.

To analyze the temperature and time dependences of topographic structure and domain potential contrast the average corrugation angle and average domain potential difference between c are a domains were determined. The time dependence of domain potential contrast on heating and cooling is shown in Fig. 2a,b. To quantify the kinetics, the time dependence of domain potential contrast, $\Delta\varphi$, was approximated by an exponential function

$$\Delta\varphi = \Delta\varphi_0 + A\exp(-t/\tau), \tag{6}$$

where τ is relaxation time and A is a prefactor. Due to the finite heating and cooling rates, the domain potential contrast immediately after the temperature change can not be reliably established; therefore, Eq. (6) describes the late stages of potential relaxation. The temperature dependence of the potential redistribution time is shown in Fig. 2c. The redistribution time is almost temperature independent with an associated relaxation energy of ~4 kJ/mole. This low value of activation energy suggests that the kinetics of relaxation process is limited by the transport of charged species to the surface. The characteristic redistribution time is ~ 20 min and is close to the relaxation time for domain potential contrast above T_c (30 min) [12].

The redistribution process both on heating and cooling results in the same equilibrium value of domain potential contrast, $\Delta\varphi_0$. The temperature dependence of domain potential contrast, shown in Fig. 2d, is almost linear, with the zero potential difference corresponding to temperature ~110°C well below the Curie temperature of $BaTiO_3$ (T_c = 130°C). For higher temperatures the degree of screening is smaller and the Coulombic contribution to the effective SSPM potential increases. Since polarization charge and screening charge contributions to the effective surface potential are of opposite sign, the decrease of the degree of screening results in the *decrease* of domain potential contrast. The thermodynamics of this process are expected to be strongly temperature dependent and to dominate over relatively weak variation of spontaneous polarization with temperature (P = 0.26 C/m^2 at 25°C and 0.20 C/m^2 at 100°C).

The equilibrium domain potential contrast can be related to the degree of screening of spontaneous polarization. As shown in Fig. 2d, the temperature dependence of equilibrium domain potential contrast in the temperature interval 30°C < T < 100°C is linear and the domain potential contrast is the same on heating and cooling, i.e. equilibrium is achieved. This dependence can be represented by the linear function $\Delta V_{dc} = 0.059 - 5.3 \cdot 10^{-4}T$, where T is temperature in Celsius degrees. Using Eq. (12) for tip length of 10 μm yields the temperature dependence of equilibrium degree of screening is

$$1 - \alpha = 1.627 \cdot 10^{-5} + 1.23 \cdot 10^{-6}T \tag{7}$$

A comparison of Eq. (3) and Eq. (7) allows us to estimate the enthalpy, ΔH_{ads}, and entropy, ΔS_{ads}, of adsorption as ΔH_{ads} = 164.6 kJ/mole, ΔS_{ads} = -126.6 J/mole K.

The enthalpy and entropy of adsorption thus obtained are within expected values in spite of the approximations inherent in this approach. The Coulombic contribution to the effective potential can be estimated as < 10-20 % thus validating our previous conclusion that the surface is completely screened at room temperature. The nature of the screening charges can not be determined from these experiments; however, these results are also consistent with the well
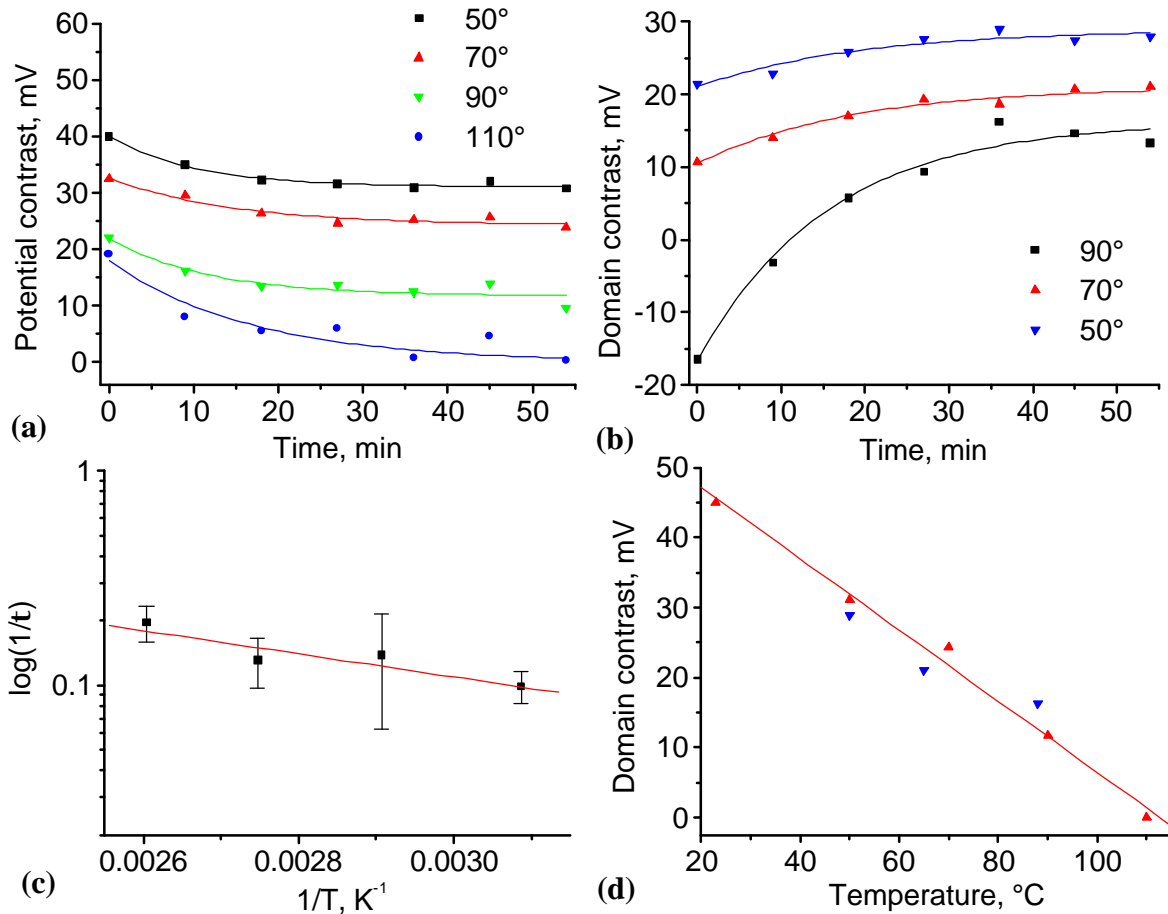
Figure 2. Time dependence of domain potential contrast on heating (a) and cooling (b). Solid lines are fits by Eq. (6) Note that on heating domain potential contrast increases and relaxes with time to some equilibrium value. On cooling the domain potential contrast reduces and in some cases change sign. Also note that the equilibrium value of domain potential contrast doesn't depend on the process. (c) Time constant for relaxation process on heating in Arrhenius coordinates and (d) temperature dependence of equilibrium domain potential contrast on heating (▲) and cooling (▼) and fit by Eq. (7) (solid line).

known fact that adsorbing on polar transition metal oxide surface in air are water and hydroxyl groups, -OH [13-15]. Dissociative adsorption of water as a dominant screening mechanism on $BaTiO_3$ surface in air was verified using temperature programmed desorption experiments on poled $BaTiO_3$ crystals [16]. Obviously, adsorbates can provide the charge required to screen the polarization bound charge, since corresponding polarization charge densities are of order of 0.25 C/m^2 corresponding to $2.6 \cdot 10^{-6}$ $mole/m^2$. For a typical metal oxide surface with characteristic unit cell size of ~ 4 Å this corresponds to the coverage of order of 0.25 mL.

Domain selective photodeposition

The domain specificity of adsorption illustrates the experimental behavior that certain chemical reactions depend on domain orientation. Photochemical reactivity and the structural properties of photodeposited metal are strongly dependent on semiconducting properties of $BaTiO_3$. Weakly n-doped/undoped ceramic material develops noticeable deposition layer in ~ 1-10 min. Heavily donor doped $BaTiO_3$ was extremely active under the irradiation and formation

C9.5.7

of hydrogen and metallic silver in the solution was observed. Photochemical activity of $BaTiO_3$ was found to be sensitive to surface conditions. Generally, as polished samples did not developed domain specific deposition patterns and thermal etching at 1200°C was necessary to achieve desired reactivity. Dependence of deposition rate on the radiation wavelength was also studied and the necessary wavelength was found to correspond to the bandgap of $BaTiO_3$ (E_g = 3.1 eV). For PZT the wavelength of radiation required for the deposition is higher (E_g = 4.1 eV).

Surface topography and corresponding piezoresponse force microscopy (PFM) images of $BaTiO_3$ surface are shown in Fig. 3a,b. While no distinct topographic features are seen in Fig. 3a, the PFM image clearly reveals a complicated lamellar domain pattern with characteristic domain size of order of ~200-300 nm. Note that a topographic defect (pore) results only in the minor alteration of domain structure and doesn't impair PFM contrast. The photodeposited metal pattern is clearly seen in Fig. 3c. After imaging, silver particles were mechanically removed and palladium was deposited on the surface; the corresponding AFM image is shown in Fig. 3d. Note that polarization distribution on the pristine surface and deposition patterns of silver and palladium are identical. Interestingly, the reactivity of the ferroelectric surface is not limited by the degree to which reaction has proceeded: removal and deposition steps can be repeated several times without the loss of reactivity. Another example of silver deposition along the lamellar domains is shown in Fig 4a. While in the most cases metal deposits in the form of nanoclusters, some conditions produce interesting particle geometries (triangular and hexagonal crystals in Fig 4b) and nanowires. The particle size was shown to be controllable by deposition time and solution concentration.

The mechanism for the domain selective photoreduction is closely related to the intrinsic screening on ferroelectric surfaces. In the absence of vacancy or step edge defects, transition metal oxide surfaces have a low density of surface states in the gap between the conduction band formed predominantly from the d states of the metal and valence band formed predominantly from oxygen p states. In ferroelectric materials, the normal component of polarization results in polarization charge density $s = \mathbf{P} \cdot \mathbf{n}$, where $\mathbf{P}$ is polarization and $\mathbf{n}$ is unit normal. For a typical material, such as $BaTiO_3$, polarization charge density can be 0.26 C/m^2 corresponding to 0.26 e^- per unit cell. In the regions with negative polarization (c^- domains) the effective surface charge becomes more negative and, therefore, band bending, increases. In the regions with positive polarization (c^+ domains) surface charge increases and can become positive with associated downward band bending. Irradiation with super band gap light results in the formation of a electron-hole pair. In ambient, the space charge field results in separation of the e-hole pair and charge accumulation on the surface, i.e. the photovoltage effect. However, on a surface immersed in a cation solution the electrons can reduce the metal cations preventing charge accumulation at the surface. Reduction is expected on positive domains, while oxidation is expected at negative domains in perfect agreement with experimental results.

This mechanism points to a significant advantage of polarization based lithography over other charge-based SPM lithographic techniques. On a ferroelectric substrate, local surface charge is due to atomic polarization and therefore is stable. The charge alters the electronic structure in a manner that can be exploited in surface interactions; therefore, the amount of deposited material is not limited by the amount of deposited charge. On high quality ferroelectric substrates, domains can be patterned with 10-20 nm resolution in feature size.

To illustrate the possibility of SPM lithography using PFM/photodeposition, a number of experiments using alternative ferroelectric materials were performed. Fig. 5a,b shows surface
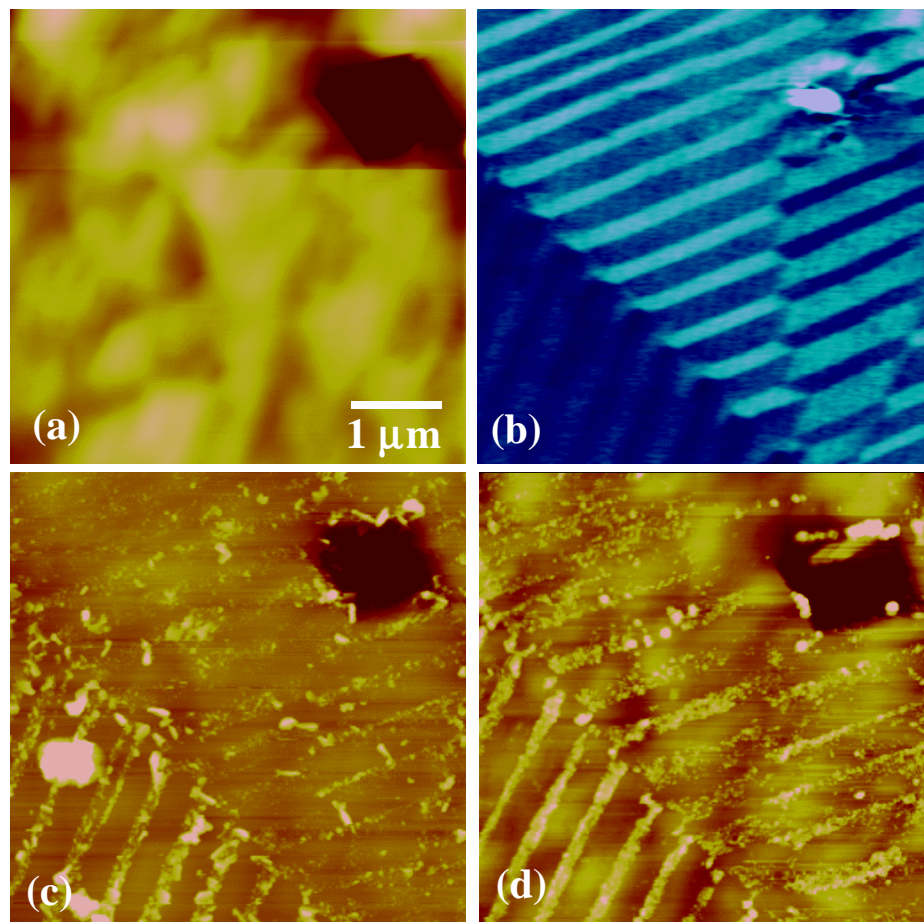
Figure 3. Local contact mode topography (a) and piezoresponse image of BaTiO$_3$ surface prior to the deposition. Topography after silver deposition (c) and palladium deposition (d). Note that the metal deposition pattern coincides with the ferroelectric domain structure as revealed bv PFM.
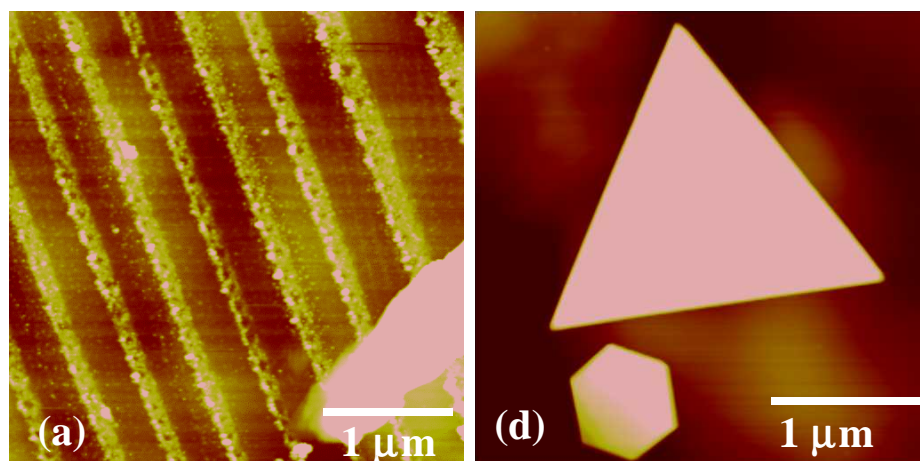
Figure 4. Silver lines (a) and gold clusters (b) on the BaTiO$_3$ surfaces.
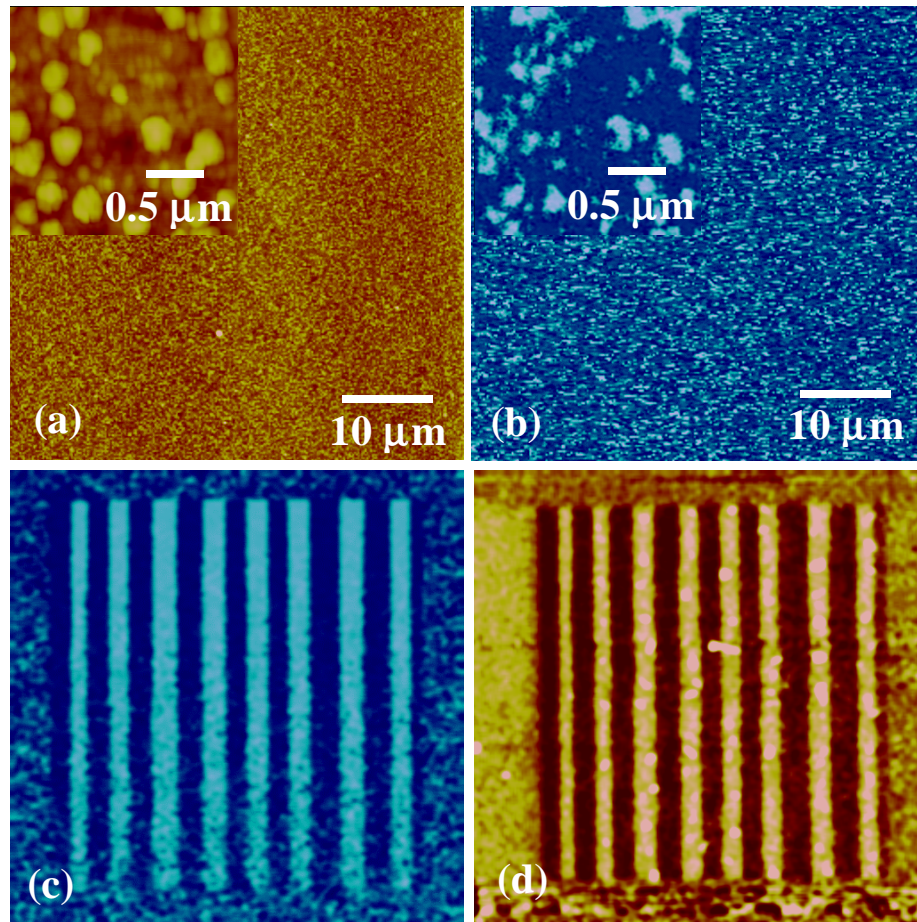
Figure 5. Surface topography (a) and piezoresponse image (b) of PZT thin film. The inset shows that the PFM contrast in not random but is due to the small (~50-100 nm) ferroelectric domains associated with grains. PFM image (c) of lines patterned with alternating +10 and -10 V_{dc}. Surface topography (d) after deposition. Note one to one correspondence between tip-induced polarization distribution and metal deposition pattern. The width of the smallest feature is ~700 nm.

topography and piezoresponse images of PZT films. The film consists of 50-100 nm grains and ferroelectric domain size is comparable with the grain size. Careful inspection of PFM images illustrates that most small grains (~50 nm) are in the single domain state, while larger grains can contain multiple domains. Unlike $BaTiO_3$ crystals, domains are small; therefore, comparison of domain structure before the photodeposition and metal deposition pattern is all but impossible. To avoid complications due to this problem, we have fabricated relatively large scale lines by the intermittent application of +10 V and -10 V to the tip. The piezoresponse image of the resulting domain pattern is shown in Fig. 5c. Image clearly illustrates the "random" polarization orientation with characteristic domain size of 50-100 nm on the edges of the image and line regions with positive or negative polarization orientation in the central part of the image. The patterned sample was placed in the silver nitrate solution and irradiated by the UV lamp for 30 min; the topographic structure is shown in Fig. 5 d. Careful inspection of the lines shows that they are formed of small (10-50 nm) silver particles. The total amount of deposited material corresponds to ~100 nm layer (comp. to the thickness of the PZT film ~ 200 nm). Therefore, reduction of silver by trapped electrons can be excluded. Note the one to one correspondence
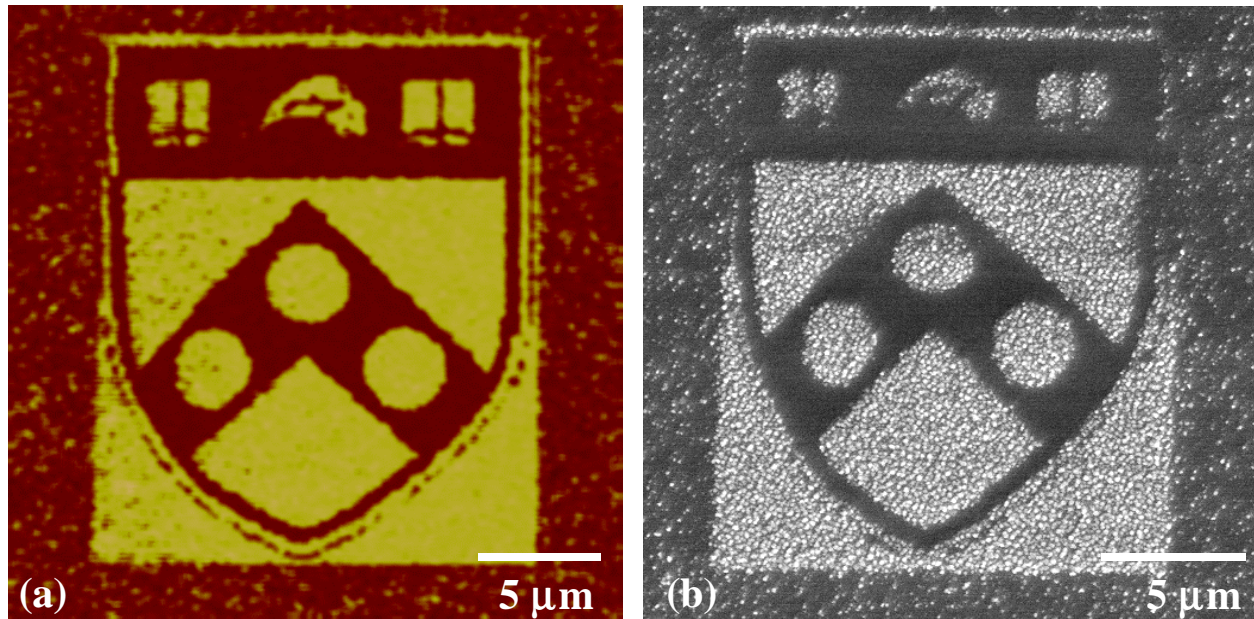
Figure 6. Piezoresponse image (a) of PZT thin film with patterned domain structure (Penn logo). SEM image (b) after deposition. Note one to one correspondence between tip-induced polarization distribution and metal deposition pattern. The grain size of Ag particles is ~ 50-100 nm and is determined by deposition time.

between the polarization pattern on the PFM image and photodeposited silver pattern. Deposition occurs exclusively on the domains written by the negative voltage, i.e. positive domains. Very little silver particle density was observed on the negative domains. The lateral size of the smallest feature on the image is ~700 nm. The lateral width of the features that can be written on PZT surface in this case is limited by the grain size of the film and was found to be 30-50 nm. Shown in Fig. 6a,b is the example of more complex polarization pattern created using PFM lithography [7] and corresponding metal photodeposition pattern.

These results illustrate the potential of controlled polarization switching with subsequent metal photodeposition for metal meso- and nanoscale structure fabrication. Obviously, polarization and deposition steps can be repeated sequentially to produce more complex nanostructures.

CONCLUSIONS

The relationship between atomic polarization and charge compensation can be exploited to induce local surface adsorption and chemical reactivity. Recent advances in scanning probe type measurements allow domain specific thermodynamic parameters of these reactions to be determined. In combination with domain patterning by local fields or e-beam lithography, reaction specificity can be used to produce complex multi-component nanostructures.

ACKNOWLEDGEMENTS

REFERENCES

1. V.M. Fridkin, *Ferroelectric Semiconductors*, (Consultants Bureau, New York, 1980).
2. J.L. Giocondi, G.S. Rohrer, *Chem. Mater*. **13**, 241 (2001).
3. J.L. Giocondi and G.S. Rohrer, *J. Phys. Chem* **B 105**, 8275 (2001).
4. M.E. Lines, A.M. Glass, *Principles and Applications of Ferroelectric and Related Materials*, (Clarendon Press, Oxford, 1977).
5. *Ferroelectric Ceramics*, Eds. N. Setter, E.L. Colla (Birkhauser Verlag Basel, 1993).
6. S.V. Kalinin and D.A. Bonnell, *Phys. Rev.* **B 63**, 125411 (2001).
7. Dmitry L. Gorbachev and E. Peng, NanoEdv2
8. S.V. Kalinin, C.Y. Johnson, and D.A. Bonnell, *J. Appl. Phys*., in print (March 2002).
9. G.A. Smolenskii, V.A. Bokov, V.A. Isupov, N.N Krainik, R.E. Pasynkov, and A.I. Sokolov, *Ferroelectrics and Related Materials* (Cordon and Breach, New York, 1984).
10. A.F. Devonshire, *Phil. Mag*. **40**, 1040 (1949).
11. A.F. Devonshire, *Phil. Mag*. **42**, 1065 (1951).
12. S.V. Kalinin and D.A. Bonnell, *J. Appl. Phys*. **87**, 3950 (2000).
13. D.A. Bonnell, *Prog. Surf. Sci*. **57**, 187 (1998).
14. C. Noguera, *J. Phys*. **C 12**, R367 (2000)
15. V.E. Henrich and P.A. Cox, *The Surface Science of Metal Oxides* (Cambridge University Press, Cambridge, 1994).
16. S. Gupta, S.V. Kalinin, and D.A. Bonnell, unpublished